Onset of initial planar instability with surface-tension anisotropy during directional solidification

Zhijun Wang, Jincheng Wang,* and Gencang Yang
State Key Laboratory of Solidification Processing, Northwestern Polytechnical University, Xi'an 710072, People's Republic of China
(Received 27 April 2009; revised manuscript received 7 September 2009; published 30 November 2009)

A simple model is presented to describe the variation of the onset of the initial planar instability with surface tension anisotropy during directional solidification. The effect of surface-tension anisotropy on the incubation time and the initial average wavelength of planar instability are predicted by the simple model quantitatively, which are also verified by phase field simulation. Investigation results reveal that surface-tension anisotropy is one of important factors in the dynamic process of planar instability. The contribution of surface-tension anisotropy to the tilting modulation is also analyzed by comparing the results from the present simple model with those from phase field simulation.

DOI: 10.1103/PhysRevE.80.052603 PACS number(s): 68.03.Cd, 81.30.Fb, 47.20.Ib

Solidification involves a complex interplay of interface dynamic and transport phenomena, which may launch complex interface morphology. During solidification, the interface morphology dominates the final material microstructures which affect the mechanical and electronical properties of materials. Therefore, the relevant problems of microstructure evolution are of interest to many physicists and metallurgists. For most metallic alloys, solidification process is dominated by solutal diffusion and/or thermal diffusion. The physical mechanism of interface instability is rooted from the competition between the destabilizing effects of the solutal diffusion and the stabilizing effects of the temperature gradient and of the surface tension [1]. The long-standing investigations on the solidification pattern formation have revealed that surface-tension anisotropy, although small, plays an important role in the microstructure evolution. Surface-tension anisotropy may significantly influence the mechanism of stability and the selective condition of free crystal growth [2–4]. During directional solidification, surface-tension anisotropy, an essential factor for the stationary cellular array, tilted cellular/dendritic array and seaweed patterns [5–10], may also compete to determine the planar interfacial stability [11–13].

Most of the previous studies concentrated on the effect of surface-tension anisotropy on pattern selection of the final steady state. However, as a dynamic process, microstructure evolution is usually affected by the evolution history during directional solidification. The cellular/dendritic array originates from the instability of the planar front. Therefore it is necessary and significant to investigate the initial planar interfacial instability, where the surface tension may also play an important role. The initial instability occurs during the initial transient stage of establishment of solutal boundary layer, where the incubation time from the beginning to the observation instability of initial microstructure and the interface morphology are of scientific and technical interests [14,15]. The time-dependent Mullins-Sekerka stability analysis was first presented by Warren and Langer to predict the onset of initial planar instability [14]. The incubation time and the initial wavelength of the initial planar instability can be well predicted by this time-dependent analysis [16]. Their stability analysis in the transient stage, however, did not take surface-tension anisotropy into account. Although the effects of surface-tension anisotropy on linear instability are widely investigated, on one hand there is no corresponding experimental or simulational proofs because of the difficulties in directly investigating the critical point of control parameters; on the other hand, the dynamic evolution process of initial planar instability with surface-tension anisotropy is seldom considered in analytical works. Herein, investigation on the onset of initial instability during the transient stage of directional solidification will supply a view to evaluate the effect of surface-tension anisotropy on the linear instability. With this method, the linear stability analysis can be quantitative verified by experiments and /or simulations. Moreover, this method also can provide a new quantitative connection between the surface-tension anisotropy and the microstructures, and then information on the surface-tension anisotropy can be obtained from the initial average wavelength.

In this Brief Report, first, a simple model is proposed to predict the dynamic planar instability process involving surface-tension anisotropy based on the time-dependent instability analysis and Fourier synthesis. Analytical results from the simple model can reveal the effect of surface-tension anisotropy on the planar instability quantitatively according to the incubation time and the initial average wavelength. Then quantitative phase field simulations are carried out to validate the simple model. Finally, the relationship between tilting modulation and surface-tension anisotropy is uncovered by comparing the results from the simple model with those from the phase field simulations.

In the experiments of directional solidification, the quasi-two-dimensional system of Hele-Shaw cell is usually considered. The cell is pulled at a constant velocity V from the hot end to the cold end. The hot end and the cold end present an external imposed thermal gradient G, corresponding to the heat flow. Using the "frozen temperature approximation," the temperature field in the cell is $T=T_M+Gz$ in the laboratory frame of reference, where T_M is the melting temperature of pure solvent and z the heat-flow direction. The concentration of solute is denoted by the far-field concentration c_∞. A typical representation of surface-tension anisotropy with fourfold symmetry is $\gamma=\gamma_0[1+\gamma_4 \cos 4(\theta+\theta_0)]$ in two dimensions, where γ_0 is the isotropic part of the surface tension, γ_4 is the anisotropic intensity of the surface tension, θ is the angle

*Corresponding author. FAX: 86-29-88491484; jchwang@nwpu.edu.cn

between the normal vector of the interface and the heat-flow direction, and θ_0 is the misorientation of preferred crystallographic orientation with the heat-flow direction. In the one-sided model, the local equilibrium at the interface gives the free boundary conditions,

$$c_S = kc_L, \tag{1}$$

$$V_n(c_L - c_S) = -D\frac{\partial c_L}{\partial z}, \tag{2}$$

$$T_I = T_M + mc_L - \kappa\Gamma[1 - 15\gamma_4 \cos 4(\theta + \theta_0)], \tag{3}$$

where c_S and c_L are concentration at solid side and liquid side of the interface respectively, k is the partition coefficient, D is the chemical diffusion coefficient, T_I is the temperature at the interface, m is the slope of liquidus line, κ is the interface curvature, $\Gamma = \gamma_0 T_M / L$, and L is the latent heat. The solutal diffusion equation and the free boundary conditions describe the directional solidification process. In the linear stability analysis, the anisotropic term of the capillary effect in Eq. (3) can be simplified as (see Appendix)

$$1 - 15\gamma_4 \cos 4(\theta + \theta_0) \approx 1 - 15\gamma_4 \cos 4\theta_0. \tag{4}$$

During the initial transient stage, concentration boundary layer can be described as [14]

$$c(z,t) = c_\infty + [c(z_I,t) - c_\infty]\exp[-2(z - z_I)/l], \tag{5}$$

where $c(z,t)$ is the time-dependent concentration field ahead of the planar front, z_I is the interface position, and l is the diffusion length. Here z_I and l are time dependent, which can be calculated from two coupled differential equations,

$$V_I = \frac{\partial z_I}{\partial t} = \frac{2D(z_I - z_\infty)}{l(1-k)z_I} - V, \tag{6}$$

$$\frac{\partial l}{\partial t} = \frac{4D(z_\infty - kz_I)}{l(1-k)z_I} - \frac{l}{z_I - z_\infty}\frac{\partial z_I}{\partial t}, \tag{7}$$

where V_I is the instantaneous interface speed and $z_\infty = mC_\infty / G$. With the time-dependent linear stability analysis, the dispersion relation of the perturbation with surface-tension anisotropy is as follows [13,14]:

$$\omega^*\left\{1 + \frac{2(z_I - z_\infty)}{l} + \frac{\Gamma[1 - 15\gamma_4 \cos(4\theta_0)]\omega^2}{G}\right\} = \frac{V_I}{D} + \frac{2(z_I - z_\infty)}{l}\left\{\frac{V_I + V}{D} + \frac{\sigma_\omega(t)}{V_I + V} + \frac{1}{z_I} + \frac{\Gamma[1 - 15\gamma_4 \cos(4\theta_0)]\omega^2}{Gz_I}\right\}. \tag{8}$$

Here $\omega^* = (V_I + V)/2D + \{\omega^2 + [(V_I + V)/2D]^2\}^{1/2}$, $z_\infty = mC_\infty / G$, and $\sigma_\omega(t)$ is the amplification rate of perturbation with space frequency ω. The Fourier synthesis method is presented as [16]

$$z_I(x,t) - z_0(t) = \sum A_\omega(t)\cos[\omega x + \phi_\omega(t)], \tag{9}$$

where $z_0(t)$ is the basic interface position, the amplitude

$$A_\omega(t) = A_\omega(0)\exp\left(\int_{t_0}^{t} \sigma_\omega(t)dt\right), \tag{10}$$

and the phase $\phi_\omega(t)$ is supposed to be stochastic in $[0, 2\pi]$ with mean distribution and $\phi_\omega(t) = \phi_\omega(t_{0-})$ after t_0, t_0 is the time when $\sigma_\omega(t)$ changes over from negative to positive. In the amplitude evolution formula, the initial interfacial fluctuation is taken as the uniform fluctuation spectrum [17,18]

$$A_\omega(0) = \frac{k_B T_M}{\gamma_0(1 - 15\gamma_4 \cos 4\theta_0)\omega^2}, \tag{11}$$

which is different from the equilibrium fluctuation spectrum as used in Ref. [16].

Combining the Fourier synthesis method and the time-dependent linear stability analysis with surface-tension anisotropy, the dynamic evolution of planar stability can be predicted. Here the numerical calculation is performed with succinonitrile-0.43 wt. % C152 at $G = 20.2$ K cm^{-1}, $V = 50$ μm/s, which has been experimental investigated in Ref. [15]. The chemical diffusion coefficient in liquid phase $D \approx 0.45 \times 10^{-9}$ m^2/s, partition coefficient $k = 0.05$, Gibbs-Thomson coefficient $\Gamma = 6.48 \times 10^{-8}$ K/m, and the slope of liquidus line $m = -542$ K/mol.

Recently the development of the phase field method with a diffuse interface makes it facilitated to investigate the microstructure evolution during solidification [19,20]. Therefore, phase field simulations are also performed for further validation of this simple model. The phase field model adopted here is presented by Echebarria *et al.* [20], which has been benchmarked by detailed numerical tests in two dimensions. The simulations are performed in two-dimension with explicit time stepping and finite differences for the spatial derivatives. The calculation domain is 1200×1000 μm^2. The diffuse interface thickness parameter in the phase field model $W = 1$ μm, $dx = 0.4$ W. During calculation, stochastic noise is imposed on the phase field across the diffuse interface to simulate the effect of fluctuations on the liquid/solid interface.

Obviously, the critical point of planar instability is affected by the surface-tension anisotropy. The surface-tension anisotropy does not influence the solutal diffusion process, but affects the interface stability by changing the boundary condition in the free boundary problem. The coupling relationship between the interface dynamics and the diffusion process indicates that the dynamic evolution of planar instability depends on the strength of surface-tension anisotropy. The simple model can quantitatively predict the planar instability with surface-tension anisotropy. The incubation time and initial average wavelength of planar instability with surface-tension anisotropy obtained from both the simple model and phase field simulation are presented in Fig. 1. Comparison of the results from the simple model and phase field simulations shows a consistent regularity on the effects of surface-tension anisotropy on planar instability: the incubation time and initial average wavelength increases as $-\gamma_4 \cos(4\theta_0)$ increases. The discrepancy of incubation time between the simple model and phase field simulations possibly originates from the selected intensity of the background

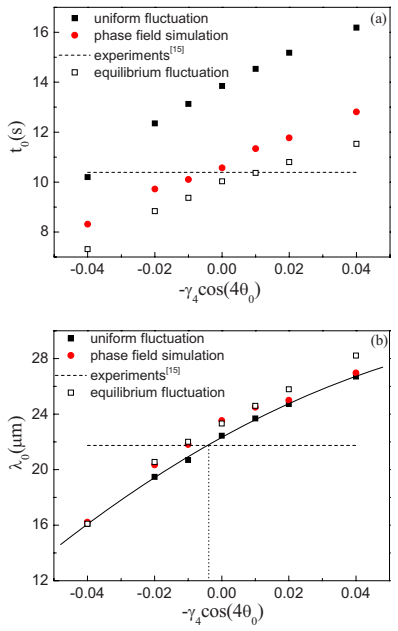

FIG. 1. (Color online) The incubation time (a) and the initial average wave (b) length with surface-tension anisotropy from the simple model and the phase field simulations.

fluctuation in the phase field simulations. As to the average wavelength, both the results from the present model and the phase field simulations agree very well with each other, which indicate that the simple model can predict the incubation time and initial average wavelength of the initial instability quantitatively.

Moreover, it is interesting to note the influence of the background fluctuation spectrum on the results, which is also shown in Fig. 1. It shows that the form of background fluctuations does not have significant influence on the initial average wavelength [Fig. 1(b)] but will change the incubation time significantly [Fig. 1(a)]. The incubation time with equilibrium fluctuation is about 28% smaller than that with uniform fluctuation; however, the discrepancy of initial average wavelength is less than 6%. The Fig. 1(a) also indicates that if the interface is less stiff, it has larger fluctuations with smaller incubation time [the smaller of $\gamma_0(1-15\gamma_4\cos 4\theta_0)$, the smaller incubation time]. As to the influence on the wave number, although the background fluctuations greatly depend on the original spectrum, the evolution of the spectrum according to the time-dependent linear stability analysis predominates during the transient stage. Therefore the background fluctuation spectrum does not influence the initial average wavelength greatly as shown in Fig. 1(b). It should be noted that, although both the uniform fluctuation spectrum and the equilibrium fluctuation spectrum show a good qualitative agreement with each other, based on the fluctuations of solidification, the simple model with uniform fluctuation spectrum has its physical footstones.

According to the above comparison, the initial average wavelength is a more independent feature, which may be a proper quantitative connection between the surface-tension anisotropy of atomic scale and the microstructure. The experimental data from Ref. [15] are also plotted in Fig. 1. In

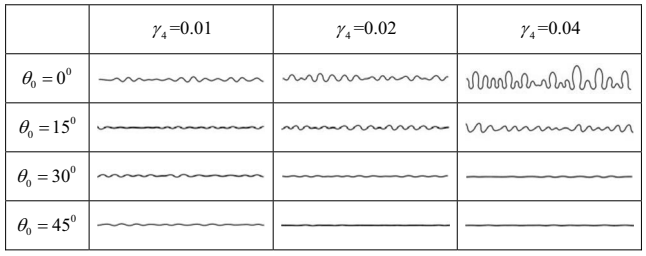

FIG. 2. The interface morphologies with surface-tension anisotropy at $t=9$ s from phase field simulations.

the experiment, the heat-flow direction is consistent with the preferred crystallographic orientation, but the anisotropic intensity of surface tension is unknown. The incubation time is counted by second in experiments and affected by the intensity of the background fluctuations, so the relative error is quite large. Therefore here the comparison of incubation time cannot provide useful information of surface-tension anisotropy. However, the initial average wavelength is insensitive to the intensity of the background fluctuation, so the intensity of surface-tension anisotropy can be determined by comparing the initial average wavelength from experiments and this simple model. In Fig. 1(b), γ_4 is estimated to be 0.004. Therefore, the intensity of surface-tension anisotropy could be evaluated by the initial average wavelength with proper and systematic experiments using the present model.

Figure 2 shows the interface morphologies with surface-tension anisotropy at $t=9$ s from phase field simulations within the width of 300 μm, where the surface-tension anisotropy influences the interface modulation obviously. As γ_4 increases with a fixed misorientation angle θ_0, the critical point of planar instability comes earlier with a smaller initial average wavelength. For a given anisotropic intensity γ_4, the dynamic evolution of planar instability is affected by the value of $\cos 4\theta_0$. The surface-tension anisotropy destabilizes the planar interface when $\cos 4\theta_0 > 0$, but stabilizes when $\cos 4\theta_0 < 0$. The incubation time for $\gamma_4=0.02$, $\theta_0=0°$ and $\gamma_4=0.04$, $\theta_0=15°$ is 9.68 s and 9.40 s, respectively; meanwhile, the incubation time for $\gamma_4=0.01$, $\theta_0=0°$ and $\gamma_4=0.02$, $\theta_0=15°$ is 10.11 s and 10.29 s, respectively. This reveals that the effect of surface-tension anisotropy on incubation time is only dependent on the multiply of γ_4 and $\cos(4\theta_0)$, which consists with the linear stability analysis with surface-tension anisotropy and also has demonstrated that the simplification of Eq. (4) is valid.

Figure 2 also shows the tilting interface morphologies with surface-tension anisotropy for $\theta_0=15°$ and $\theta_0=30°$. However, this kind of tilting growth cannot be predicted by the simple model. In the linear stability analysis, the surface-tension anisotropy is shown to be irrelevant to the tilting growth but the anisotropic kinetics is responsible to the effect [10–12]. The present simple model is also based on the linear analysis; therefore, it cannot predict the tilting modulation as shown in Fig. 2. However, previous simulation results and experimental investigations indicate that the surface-tension anisotropy may be relevant for the fully nonlinear regime [5–9]. The planar instability for $\theta_0=15°$ and $\theta_0=30°$ in Fig. 2 indicates the responsibility of surface-

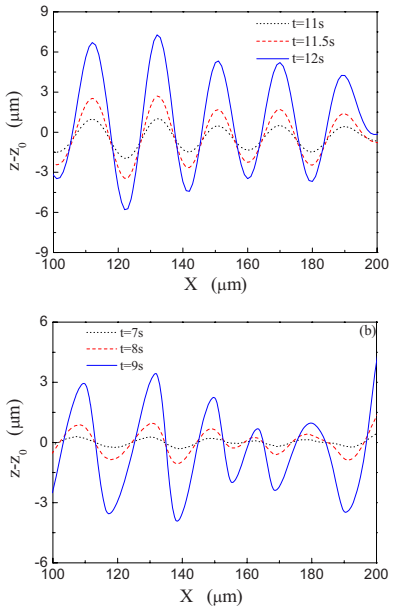

FIG. 3. (Color online) The dynamic evolution of planar instability with $\gamma_4=0.04$, $\theta_0=15°$ (a) from the simple model, (b) from phase field simulations.

tension anisotropy for tilting growth. To clarify the tilting growth in details, Fig. 3 shows the dynamic process of planar instability before onset of planar instability obtained from both the simple model [Fig. 3(a)] and phase field simulations [Fig. 3(b)]. The wave number in Fig. 3 is almost constant after modulation appears, which is the reason of that the present model can predict the initial average wavelength very well even it cannot explain the tilting growth. The interface modulation is well-balanced without leaning to the right side at earlier. As time increases, the amplitude of modulation enlarges. During the amplification, the tip point moves to right and the bottom point moves to left, which result in the tilting morphology in the phase field simulation. For the interface morphology from the simple model, the modulation is still normal without lean. It can be inferred that the tilting modulation do not appear at the early instability stage. In the linear growth regime, the anisotropic surface tension does not lead to the tilting grow, while in the nonlinear growth regime, the misaligned orientation of surface-tension anisotropy does induce the traveling-wave modulation after the planar interface instability.

To summarize, a simple model with surface-tension anisotropy based on the time-dependent linear stability analysis is proposed, which can predict the incubation time and the initial average wavelength very well except the tilting growth onset of initial planar instability. Phase field simulations validate the results from the simple model and clarify that the surface-tension anisotropy can induce tilting growth in the nonlinear growth regime of planar instability. Investigations on the onset of initial planar instability with surface-tension anisotropy reveal that the crossover point of planar instability and the initial microstructure are strongly influenced by the surface-tension anisotropy. The tilting growth appears at the onset of the initial planar instability due to the nonlinear effect of misaligned orientation of surface-tension anisotropy with heat flow.

The work was supported the fund of the State Key Laboratory of Solidification Processing in NWPU, China (Grants No. 17-TZ-2007, No. 03-TP-2008, and No. 24-TZ-2009) and the Doctorate Foundation of Northwestern Polytechnical University.

APPENDIX

In the boundary condition with surface-tension anisotropy

$$\cos 4(\theta+\theta_0)=\cos 4\theta\cos 4\theta_0-\sin 4\theta\sin 4\theta_0. \quad \text{(A1)}$$

With infinitesimal perturbation on the planar interface

$$(\cos\theta)^2=1+h_x^2, \quad \text{(A2)}$$

$$\cos 4\theta=2(\cos 2\theta)^2-1=2[2(\cos\theta)^2-1]^2-1$$
$$=1+8(\cos\theta)^4-8(\cos\theta)^2, \quad \text{(A3)}$$

where h_x^2 is a higher order infinitely small quantity. Therefore in the linear instability analysis $\cos 4\theta$ can be taken for one and then $\sin 4\theta$ is zero.

[1] W. W. Mullins and R. F. Sekerka, J. Appl. Phys. **35**, 444 (1964).
[2] M. Ben Amar and Y. Pomeau, Europhys. Lett. **2**, 307 (1986).
[3] A. Barbieri, D. C. Hong, and J. S. Langer, Phys. Rev. A **35**, 1802 (1987).
[4] J. J. Xu, Phys. Rev. E **53**, 5051 (1996).
[5] S. Akamatsu, G. Faivre, and T. Ihle, Phys. Rev. E **51**, 4751 (1995).
[6] T. Okada and Y. Saito, Phys. Rev. E **54**, 650 (1996).
[7] S. Akamatsu and G. Faivre, Phys. Rev. E **58**, 3302 (1998).
[8] B. Utter, R. Ragnarsson, and E. Bodenschatz, Phys. Rev. Lett. **86**, 4604 (2001).
[9] J. Deschamps, M. Georgelin, and A. Pocheau, Europhys. Lett. **76**, 291 (2006).
[10] J. Deschamps, M. Georgelin, and A. Pocheau, Phys. Rev. E **78**, 011605 (2008).
[11] S. R. Coriell and R. F. Sekerka, J. Cryst. Growth **34**, 157 (1976).
[12] R. B. Hoyle, G. B. McFadden, and S. H. Davis, Philos. Trans. R. Soc. London, Ser. A **354**, 2915 (1996).
[13] Z. J. Wang, J. C. Wang, and G. C. Yang, Cryst. Res. Technol. **44**, 43 (2009).
[14] J. A. Warren and J. S. Langer, Phys. Rev. E **47**, 2702 (1993).
[15] W. Losert, B. Q. Shi, and H. Z. Cummins, Proc. Natl. Acad. Sci. U.S.A. **95**, 431 (1998).
[16] Z. J. Wang, J. C. Wang, and G. C. Yang, Appl. Phys. Lett. **94**, 061920 (2009).
[17] A. Karma, Phys. Rev. E **48**, 3441 (1993).
[18] J. J. Hoyt, M. Asta, and A. Karma, Mater. Sci. Eng. R. **41**, 121 (2003).
[19] W. J. Boettinger, J. A. Warren, C. Beckermann, and A. Karma, Ann. Rev. Mater. Res. **32**, 163 (2002).
[20] B. Echebarria, R. Folch, A. Karma, and M. Plapp, Phys. Rev. E **70**, 061604 (2004).